Pak. j. sci. ind. res. Ser. A: phys. sci. 2019 **62A**(2) 67-75

Facile Synthesis and Characterization of Wollastonite Polyindole Composites to Study their Electrical Conductivity Behaviour

Khalid Javed[a]*, Farah Kanwal[a], Saadat Anwar Siddiqi[b], Shahid Atiq[c], Waheed Mushtaq[a] and Khalil Ahmed[a]

[a]Institute of Chemistry, University of the Punjab, Lahore, Pakistan
[b]Interdisciplinary Research Centre in Biomedical Materials, COMSATS IIT, Lahore, Pakistan
[c]Centre of Excellence in Solid State Physics, University of the Punjab, Lahore, Pakistan

(received August 7, 2018; revised September 26, 2018; accepted December 4, 2018)

Abstract. In this work pure polyindole and its composites with wollastonite have been prepared by using anhydrous ferric chloride ($FeCl_3$) as an oxidizing agent. Wollastonite ($CaSiO_3$) was prepared by sol gel method using citric acid, calcium nitrate and tetraethylorthosilicate (TEOS) for the synthesis of composites. Particle size of the synthesized wollastonite was 58.8 nm. Effect of wollastonite weight percentages ranging from 1-25% of the polyindole in polyindole wollastonite (PIn/$CaSiO_3$) composites was studied. Chemical structure was elucidated for polyindole/wollastonite (PIn/$CaSiO_3$) composites and wollastonite ($CaSiO_3$) was done through Fourier transform infra red spectroscopy (FTIR), which revealed successful fabrication of polyindole/wollastonite (PIn/$CaSiO_3$) composites and wollastonite ($CaSiO_3$) particles. Scanning electron microscopic technique was used for surface morphological studies. Thermal stability of the composites was examined through thermogravimetry. Four probe method was used to measure DC-conductivity of the samples. Composites showed DC conductivity in the range, 3.71×10^{-7} Siemens per centimeter.

Keywords: wollastonite, polyindole, composites, conductivity, thermal stability

Introduction

In recent years, a lot of attention has been paid to the polymer base conducting composites due to their significant applications in various fields such as digital devices, fuel cells, chemical sensors, electrochromic displays, capacitors, anti-corrosion coatings, pharmacology, neuron treatment and batteries as reported by Moraes *et al*. (2004); Kan *et al*., (2004) and Oyama *et al*. (1995). Bartlett and Farrington (1992) and Skotheim (1986) reported that heterocyclic conducting polymers such as polypyrrole, polythiophene, polyaniline, polycarbazole and polyindole are of prime importance due to their electroactive features. Among these conducting polymers, poly(paraphenylene) and polypyrrole are suggested/recommended as good electrical conductors with long range thermal stability. But, indole monomer has both pyrrole and aromatic ring. So, the polyindole polymer has conducting characteristics. However, polyindole and its composites have been explored very infrequently among aromatic conducting polymers as reported by Billaud *et al*. (1995); Tourillon and Garnier (1982). Zhijiang *et al*. (2012) reported that now a days, polyindole and its composites have been promoted in various domains such as battery and conducting electrodes. Polyindole is well known due to its redox property and environment stability which motivates its applications in secondary batteries. It is proposed that in polyindole protons are used as a charge carrier to enhance the electrical conductance. However, the doping of various metal ions and salts in polyindole can increase the electrical conductivity.

Sainz *et al*. (2010) reported that numerous clays, oxides, chlorides and sulphides can be added in polyindole to achieve composites of required features. Wollastonite ($CaSiO_3$) is an inorganic material composed of oxides of calcium (CaO) and silicon (SiO_2). Maxim and McConnell (2005) described that wollastonite is a naturally occurring mineral having multiple significant electrical and biological properties. Due to high bioactivity and non-toxicity, calcium silicate has wide range of applications as a bone substitute in biomedical field and repairing of neurons in the form of composites (Wei *et al*., 2009; Chakradhar *et al*., 2006). Wollastonite show minimum thermal expansion, chemical inertness, thermally stable, creep resistance, high temperature stability and good electrical conductance (Zhao *et al*., 2006). In our reported work, powder of wollastonite was prepared by hydrolysis method using calcium nitrate tetra hydrate, TEOS and citric acid as precursors.

*Author for correspondence; E-mail: khalidpcsir@gmail.com

Polyindole was prepared using chemical oxidation method. Finally, the effect on electrical conductivity of various percentages of wollastonite (1-25%) on polyindole was noted by four probe methods.

Materials and Methods

Indole monomer (Uni-Chem), chloroform (BDH), Ferric chloride, $FeCl_3.6H_2O$ (Sigma-Aldrich), calcium nitrate, $Ca(NO_3)_2.4H_2O$ (Fisher), citric acid anhydrous (Sigma-Aldrich), silver nitrate (Sigma-Aldrich), Tetra ethyl orthosilicate, ammonia (Uni-Chem), potassium dichromate (Sigma-Aldrich), hydrochloric acid, nitric acid, ethyl alcohol and methyl alcohol were of pure analytical grade. During the whole experiment double distilled and deionized water was used.

Synthesis of polyindole. Polyindole was chemically synthesized by oxidation of indole using anhydrous ferric chloride which acts as an oxidizing agent. The ratio between monomer to oxidizing agent was taken as 2.5. Chloroform was employed as a solvent. Anhydrous ferric chloride was dissolved in 60 mL of chloroform. 10 mL of deionized water was added to accelerate the reaction. Indole was dissolved in 16 mL chloroform. The indole solution was added drop wise into the flask containing oxidizing agent at 15 °C. The appearance of a dark red colour indicated the onset of polymerization. Reaction mixture was continuously stirring using a magnetic stirrer. After 5 h continuous stirring by magnetic stirrer, the product was washed with warm water and filtered by vacuum filtration to obtain green coloured precipitates of polyindole. At the end, dark green coloured precipitates were washed with ethyl alcohol multiple times. Product obtained was dried in an oven at 70 °C for 24 h. The final product was grinded (Oz *et al*., 2008).

Synthesis of wollastonite. Wollastonite was synthesized using hydrolysis method from calcium nitrate ($Ca(NO_3)_2.4H_2O$), TEOS, and citric acid ($C_6H_8O_7H_2O$) as reactants. Firstly, stoichiometric amount of citric acid and calcium nitrate were dissolved sequentially in deionized water. Tetra ethyl orthosilicate (TEOS) was added slowly drop wise into the solution at room temperature under constant stirring for 10 min. Molar ratio of $Ca(NO_3)_2.4H_2O$ and TEOS was 1:1. The pH of the reaction mixture was kept at 1 by the addition of concentrated nitric acid to increase the rate of hydrolysis of TEOS. The solution was continuously stirred for 90 min at a temperature of 40 °C. A thick gel was formed which was dried at 100 °C for seven hours. The gel was decomposed at 400 °C for 2 h in muffle furnace. The resultant product was calcined at 900 °C for 2 h to obtain a white powder of wollastonite which was further analyzed by powder XRD (Anjaneyulu and Sasikumar, 2014).

Synthesis of polyindole wollastonite composites. Synthesis involved chemical oxidative polymerization of indole using anhydrous ferric chloride. The ratio between monomer to oxidizing agent was 2.5. Anhydrous ferric chloride was dissolved in chloroform. 10 mL of deionized water was added to accelerate the reaction. Various percentages of wollastonite 1-25% were added to the reaction mixture. The solution was stirred 20 min. Indole solution in chloroform was added and the appearance of dark red coloration indicated polymerization of indole. Temperature was kept at 15 °C and the reaction mixture was stirred for 5 h. After stirring for 5 h, the contents were filtered, washed with hot water until filtrate becomes colourless. A dark green coloured, polyindole composite was obtained and dried in an oven at 70 °C for 48 h.

Characterization. The crystalline phase identification and purity of wollastonite was carried out by Bruker D8 Advance X-ray diffractometer, using copper Kα (1·5406 Å) and nickel filtered radiation. The conversion of indole monomer to polyindole and formation of its composites with $CaSiO_3$ was confirmed by FTIR spectrometer (Shimadzu-6400, Japan). The morphology images of wollastonite and its composites were recorded by Scanning Electron Microscope (Hitachi S-3400N Model) at an accelerating voltage of 15 kV. The thermodynamic stability of pure wollastonite and polyindole wollastonite composites was studied by the thermogravimetric analyzer (TGA) and differential scanning calorimetry (DSC). The induced effect on electrical conductivity of polyindole was recorded by four probe conductivity apparatus.

Results and Discussion

Fourier transform infrared spectroscopy. In Fig. 1 FTIR spectra of the wollastonite shows the region 3,500/cm and 1,639/cm due to stretching and the bending vibration, respectively of O–H groups present as moisture content in the sample. The peak at 864 is absent which is the characteristic peak of calcium nitrate. The absorption band at 1091/cm signifies the asymmetrical stretching vibrations of OT-Si-OT (OT representing the

bridging oxygen) group; the absorption bands at 1016/cm represent the asymmetrical stretching vibrations of Si-OT-Si group; the absorption bands at 509/cm represent the bending vibrations of Si-OB group; the addition of FTIR absorption bands at about 799 and 1160-1250/cm from the products provide an evidence that the degree of order of amorphous silica formed by the acidolysis of wollastonite is gradually improved as the time increased from 0 to 60 min (Tangboriboon *et al*., 2011). The strong peaks indicated single-phasic wollastonite without any minor phases (Bakan *et al*., 2013).

The FTIR spectrum of the polyindole is shown in Fig. 2. The peak observed at 3440/cm corresponding to N–H stretching, which confirms that the polymerization occurred at 2 and 3 positions of monomer. This reveals that the nitrogen atom holding moiety is not involved in the formation of polyindole process. A peak obtained at 2930/cm attributed to the C–H bond of indole moiety. A peak observed at 1580/cm recognized as –NH is stretching vibrations. Small peaks at 1627 and 1530/cm correspond to the aromatic -C=C- double bond. A small peak at 742/cm indicates that the benzene ring is not involved in polymerization. The peak noticed at 1400/cm resembles to C–H stretching vibrations of the benzene ring. The narrow peaks observed at 1330 and 1050/cm designate the stretching mode of pyrrole ring and vibration mode of C–N bond. It was noticed that a peak present at 722/cm at the polymerization site of the indole monomer was disappeared after polymerization which distinguishes monomer from polymer (Gupta *et al*., 2010; Talbi *et al*., 1997). Figure 3 shows the FTIR spectra of polyindole/wollastonite composite. The FTIR spectra of composites show all the characteristic vibrations of polyindole, and wollastonite which have been shifted and confirm the formation of composites.

X-ray diffraction. XRD spectra of polyindole, wollastonite and its composites with polyindole are shown in Fig. 4. In Fig. 4A peaks observed at 20.0° and 26.4° (2θ) values corresponds to polyindole (Handore *et al*., 2014). The XRD pattern of PIn displayed broad diffraction peaks, which shows that the PIn was amorphous (Taylan *et al*., 2010). The Fig. 4B shows XRD pattern of pure wollastonite obtained after calcination at 900 °C for 8 h. A sharp peak is observed at 2θ value 29.49° in Fig. 4B, which corresponds to the indexing of XRD peaks of wollastonite matching with JCPDS data (File #043-1460). The XRD spectrograph shows the major reflections between 26 to 70° (2θ values), indicates more crystalline regions in the wollastonite. The presence of single phase with monoclinic geometry of wollastonite is confirmed (Lakshmi *et al*., 2013). A sharp peak in XRD diffractogram is the measure of crystallinity of the component,

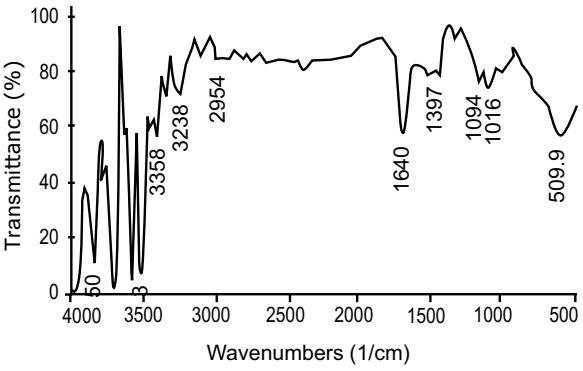

Fig. 1. FTIR spectra of pure wollastonite.

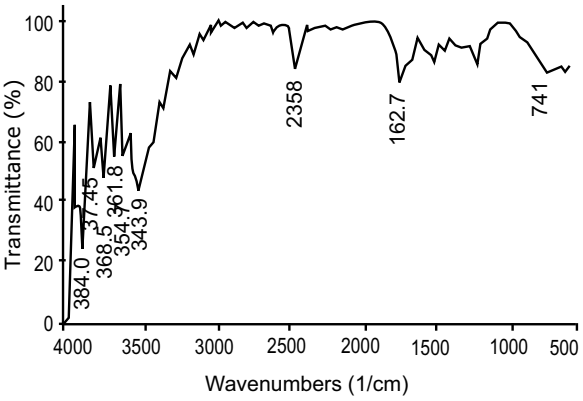

Fig. 2. FTIR spectra of pure polyindole (PIn).

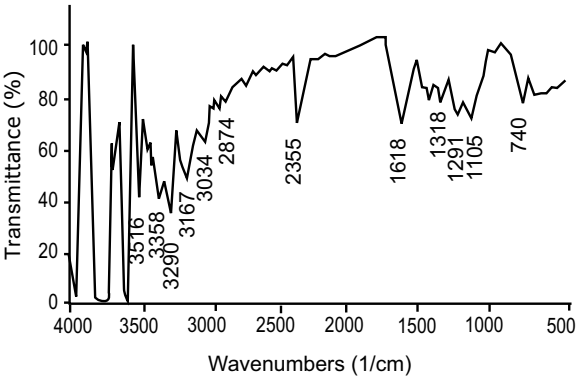

Fig. 3. FTIR spectra of pure polyindole (PIn) wollastonite composite.

higher the degree of regularity, higher is the crystallinity (Banerjee and Chattopadhyay, 2005). The average crystallite size (D) of synthesized wollastonite was calculated using Scherrer's formula (Patterson, 1939):

$$D = k\lambda/B \cos\theta \quad \ldots\ldots\ldots\ldots\ldots\ldots\ldots\ldots \quad 1$$

where:

the λ is 1.54A° which is the wavelength of Cu Kα radiation, k is the shape factor, whose value is 0.89 if shape is unknown and 1.0 for spherical crystallites, Cosθ is the cosine of Bragg's angle, and β is the half height of the diffraction angle in radians. Sharp peak at 2θ = 29.49A° which is the characteristic peak of wollastonite was chosen to calculate the average diameter. The calculated average crystallite size of the calcined wollastonite nanopowder was 58.8 nm. The lattice parameter values calculated from XRD pattern are a = 15.4301 A°, b = 7.3242 A°, c = 7.0717 A°. However, XRD spectra of polyindole wollastonite composite (Fig. 4C), shows reflections between 24-30° 2θ values which indicates high crystal-like regions in wollastonite and less intense peaks observed at 32, 34, 41, 43, 46 and 48 (2θ values) indicate amorphous behavior of polyindole wollastonite composites. Same indexing was noted as shown in Fig. 4B. The addition of polyindole change the intensity of diffraction peaks which means the crystallinity of wollastonite has been affected to some extent (Kato *et al*., 1998). The particles size of wollastonite has been increased in composites due to coating of wollastonite particles with polyindole (Chulliyote *et al*., 2017) and shows broad peak thus exhibits amorphous behavior (Taylan *et al*., 2010).

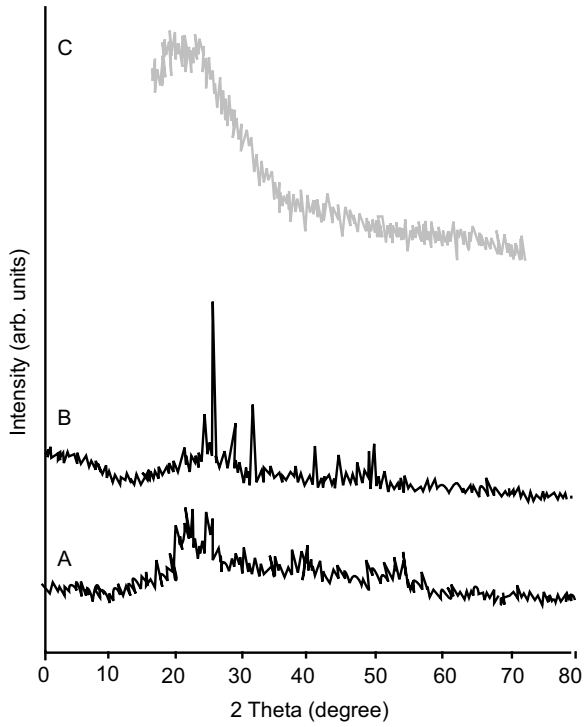

Fig. 4. X-ray diffraction patterns of the pure PIn (A) wollastonite (B) and its composites with polyindole (C).

Scanning electron microscopy. SEM images of chemically synthesized polyindole, wollastonite and polyindole wollastonite composites containing (1 to 25% of wollastonite) have been shown in Fig. 5A-G. The SEM micrograph of polyindole (Fig. 5A) shows a sponge like, porous, granular structure which is in consistent with literature (Taylan *et al*., 2010). Particle size in pure polyindole ranges between 43-85 nm with pore size 57-72 nm. Figure 5B, shows that the sample is acicular wollastonite crystals with an average length-diameter ratio of 3-5 µm or so, the fibre is entangled forming a nest-like sphere-shaped aggregates Fig. 5C (Wu *et al*., 2013). The void or pores in the product are due to release of gases (Huang and Chang, 2009). The introduction of small amount of wollastonite into polyindole caused its particles to aggregate in the form of clusters at a micrometric scale with many air gaps among the clusters (Fig. 5D). However, with increase in the amount of wollastonite (Fig. 5E-G), it is seen particle size of polypyrrole has been increased and pore size is decreased from 200-225 nm and 48-60 nm, respectively. This is because wollastonite particles are coated with the polypyrrole (Ong *et al*., 2008). Thus, well-dispersed having smooth surface composites were observed, indicating an improved interaction between the nanoparticle and the polymer (Rajasudha *et al*., 2010). Since there is a variation in grain size accompanied with porosity and compactness has been observed which has a major effect on the conductivity behavior of the polyindole composites (Ajamein and Haghighi, 2016; Aruna and Mukasyan, 2008).

Thermal analysis. TGA and DSC images of wollastonite and its composites with polyindole are shown in Fig. 6. In TGA curve of wollastonite as shown in Fig. 6a, a negligible weight loss ~5.134% was noted from 0 to 190 °C which is due to the evaporation of moisture from the wollastonite surface. A sharp percentage weight loss of 12% occur from 190-400 °C due to removal of gases like CO, CO_2 and ammonia. At 400 to 1200 °C nitrogen particles present are removed

as NO_2 showing the presence of polyindole and the decomposition of $Ca(NO_3)_2$ as impurity in the composites samples. DSC curve of pure wollastonite sample and its composite display sharp endothermic peak at 45.08 °C and 48.68 °C, respectively due to the removal of water molecules. While a broad endothermic peak was observed at ~430 °C which is due to the loss of nitrates (Wang *et al*., 2008). From TGA–DSC curve of pure wollastonite sample, thus at 880 °C a complete phase formation was observed. As no change was observed

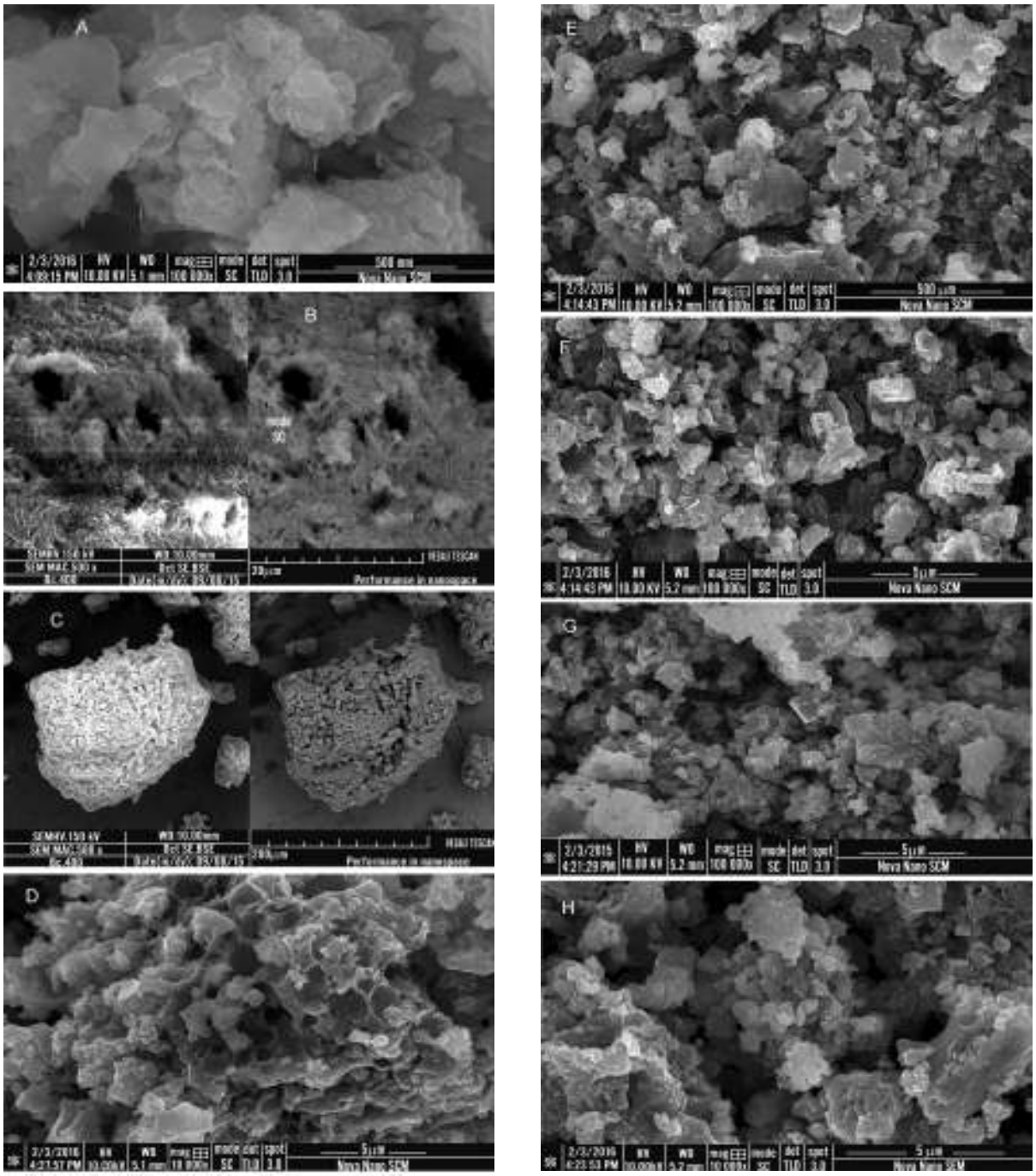

Fig. 5. SEM images of polyindole (A), wollastonite (B & C), and their composites 5% (D), 10% (E), 15% (F), 20% (G) and 25% (H).

in TGA-DSC curve after 900 °C, so the calcination temperature of wollastonite was 900 °C.

Elemental analysis. Chemical composition of wollastonite is 48.3% of CaO and 51.7% of SiO_2 (Virta and Van Gosen, 2001). The chemical analysis results of wollastonite are given in Table 1 and shown in Fig. 5. Table 1 shows that chemical composition of synthesized wollastonite is very close to its stoichiometric composition, suggesting this sample is similar to pure wollastonite, with SiO_2 and CaO very close to the theoretical $CaSiO_3$ composition (Hedström, 2006, Xinhai Sr, 2006; Rieger and Virta, 1999).

Table 1. The chemical analysis of wollastonite sample (%)

Elements	Weight (%)	Atomic (%)
C	8.03	14.07
O	44.57	58.62
Si	10.07	8.07
Ca	36.63	19.24
Total	100.00	

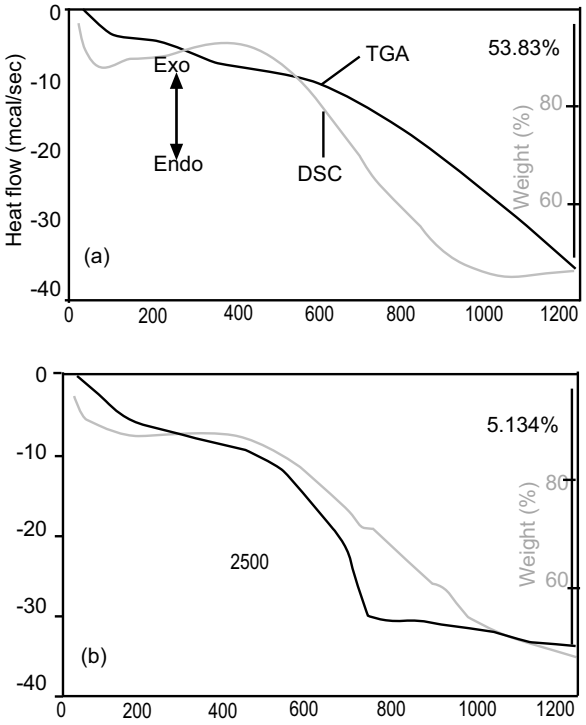

Fig. 6. TGA study of pure wollastonite (a) and its composite with polyindole (b).

Conductivity of wollastonite PIn composite. The PIn-composite powder sample was pressed to form pellets having 13 mm diameter. Conductivity measurements were made using four - probe technique. Current–voltage behavior was used to determine resistances and finally electrical conductivity of the pellets was calculated. The electrical conductivity of PIn–wollastonite composite measured at room temperature was 3.7×10-7S/cm. When conducting polymers are within the openings of meso or microporous silicates, the conductivity of polymer composites increases with an increase in ceramic material. Maximum conductivity was found with 10% ceramic material and then decreased, thus conductivity of the composite is changed from insulating behavior to conductors (Martínez *et al*., 2011).

The electrical conductivity of the PIn composite is more prominent than pure polymer chemically synthesized, the higher electrical conductivity of PIn-Ca hosts may

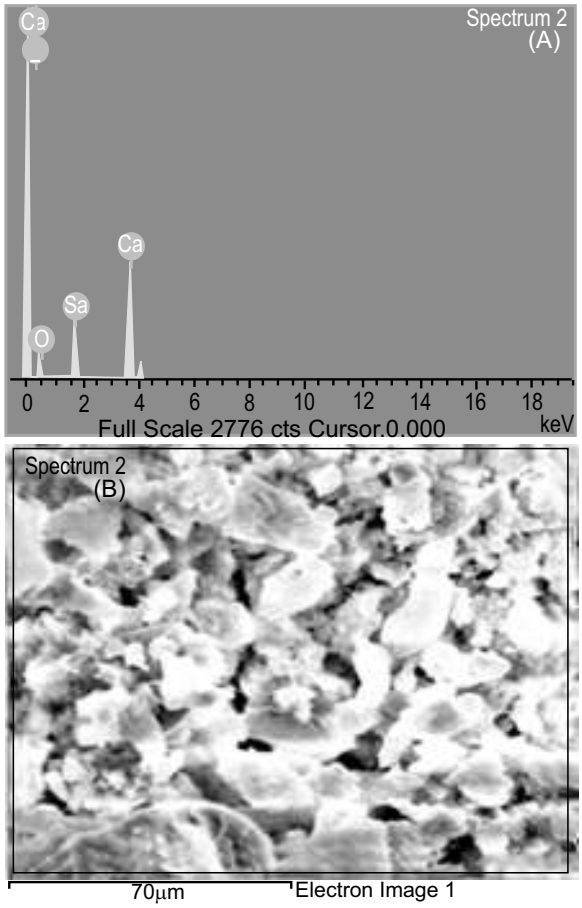

Fig. 7. The chemical analysis results of the wollastonite sample.

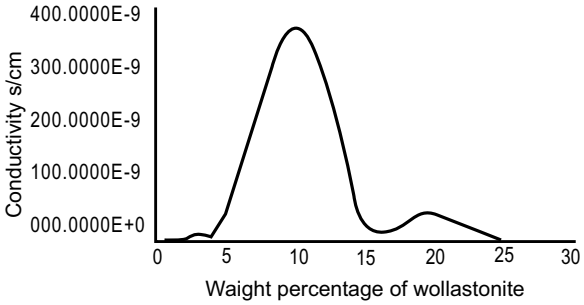

Fig. 8. Variation of conductivity with changing %age of wollastonite in composite.

be because calcium silicates, instead of silicates, influence the electrical conductivity. This performance can be attributed because Ca-hosts increase the transmission of the electrical charges from side to side of PIn chains in the openings (Costa *et al*., 2012).

Conclusion

Dark green powder of polyindole (PIn) and polyindole wollastonite (PIn/$CaSiO_3$) composites was successfully synthesized at 15 °C using anhydrous ferric chloride ($FeCl_3$) as an oxidizing agent. Wollastonite used for the composite fabrication was successfully prepared using calcium nitrate, citric acid and tetraethylorthosilicate (TEOS) using combustion synthesis. Polymerization was carried out at 15 °C and observed during the reaction by the appearance of dark red coloration which is an indication to the onset of polymerization. It occurred only at 15 °C. Structure elucidation of polyindole (PIn), wollastonite ($CaSiO_3$) and poly-indole/wollastonite (Pln/$CaSiO_3$) composites was done by Fourier transform infrared spectroscopy (FTIR) through characteristic absorption bands confirming the same chemical structure as mentioned in literature. Thermal studies of composites and pure polymer were compared. An increase in thermal stability of composites occurred which is attributed to greater weight loss in the composite material because of addition of wollastonite ($CaSiO_3$) particles of crystalline nature. Conductivity of composites increased by the addition of wollastonite ($CaSiO_3$) particles. As the amount of wollastonite ($CaSiO_3$) increased, conductivity went on further increasing trend. Surface morphological studies were done through scanning electron microscopy (SEM) images, white colored wollastonite ($CaSiO_3$) particles appeared in circular shape. In composites some particles of irregular shape were observed at the surface. On the whole polyindole/wollastonite (Pln/$CaSiO_3$) composites showed a conducting behavior as for other conducting polymers.

Conflict of Interest. The authors declare no conflict of interest.

References

Ajamein, H., Haghighi, M. 2016. On the Microwave enhanced combustion synthesis of CuO–ZnO–Al_2O_3 nano catalyst used in methanol steam reforming for fuel cell grade hydrogen production: effect of microwave irradiation and fuel ratio. *Energy Conversion and Management*, **118:** 231-242.

Anjaneyulu, U., Sasikumar, S. 2014. Bioactive nanocrystalline wollastonite synthesized by sol–gel combustion method by using eggshell waste as calcium source. *Bulletin of Materials Science*, **37:** 207-212.

Aruna, S.T., Mukasyan, A.S. 2008. Combustion synthesis and nanomaterials. *Current Opinion in Solid State and Materials Science*, **12:** 44-50.

Bakan, F., Lacin, O., Sarac, H. 2013. A novel low temperature sol–gel synthesis process for thermally stable nano crystalline hydroxyapatite. *Powder Technology*, **233:** 295-302.

Banerjee, A., Chattopadhyay, K. 2005. Recent developments in the emerging field of crystalline P-type transparent conducting oxide thin films. *Progress in Crystal Growth and Characterization of Materials*, **50:** 52-105.

Bartlett, P., Farrington, J. 1992. Electrochemically polymerised films of 5-carboxyindole: preperation and properties. *Journal of the Chemical Society Faraday Transaction*, **8:** 208-211.

Billaud, D., Maarouf, E., Hannecart, E. 1995. Chemical oxidation and polymerization of indole. *Synthetic Metals*, **69:** 571-572.

Chakradhar, R.S., Nagabhushana, B., Chandrappa, G., Ramesh, K., Rao, J. 2006. Solution combustion derived nanocrystalline macroporous wollastonite ceramics. *Materials Chemistry and Physics*, **95:** 169-175.

Chulliyote, R., Hareendrakrishnakumar, H., Raja, M., Gladis, J.M., Stephan, A.M. 2017. Enhanced cyclability using a polyindole modified cathode material for lithium sulphur batteries. *Sustainable Energy and Fuels*, **1:** 1774-1781.

Costa, M.B.G., Juárez, J.M., Martínez, M.L., Cussa, J., Anunziata, O.A. 2012. Synthesis and characterization of a novel composite: polyindole included in nanostructured Al-MCM-41 material. *Microporous and Mesoporous Materials*, **153:** 191-197.

Gupta, B., Chauhan, D., Prakash, R. 2010. Controlled morphology of conducting polymers: formation of nanorods and microspheres of polyindole. *Materials Chemistry and Physics*, **120:** 625-630.

Handore, K.N., Bhavsar, S.V., Pande, N., Chhattise, P.K., Sharma, S.B., Dallavalle, S., Gaikwad, V., Mohite, K.C., Chabukswar, V. V. 2014. Polyindole-ZnO nanocomposite: synthesis, characterization and heterogeneous catalyst for the 3,4-dihydropyrimidinone synthesis under solvent-free conditions. *Polymer-Plastics Technology and Engineering*, **53:** 734-741.

Hedström, A. 2006. Reactive Filter Materials for Ammonium and Phosphorus Sorption in Small Scale Wastewater Treatment. 47 pp., *PhD. Thesis*, Lulea University of Technology, Sweden.

Huang, X.-H., Chang, J. 2009. Synthesis of nanocrystalline wollastonite powders by citrate–nitrate gel combustion method. *Materials Chemistry and Physics*, **115:** 1-4.

Kan, J., Pan, X., Chen, C. 2004. Polyaniline–uricase biosensor prepared with template process. *Biosensors and Bioelectronics*, **19:** 1635-1640.

Kato, M., X-sen, Bunseki, B. 1998. *X-ray Spectrochemical Analysis*, 152 pp., Uchida Rokakuho Pub. Co. Ltd., Tokyo, Japan.

Lakshmi, R., Velmurugan, V., Sasikumar, S. 2013. Preparation and phase evolution of wollastonite by sol-gel combustion method using sucrose as the fuel. *Combustion Science and Technology*, **185:** 1777-1785.

Martínez, M.L., D'amicis, F.A.L., Beltramone, A.R., Costa, M.B.G., Anunziata, O.A. 2011. Synthesis and characterization of new composites: PANI/Na-AlSBA-3 And PANI/Na-AlSBA-16. *Materials Research Bulletin*, **46:** 1011-1021.

Maxim, L.D., Mcconnell, E. 2005. A review of the toxicology and epidemiology of wollastonite. *Inhalation Toxicology*, **17:** 451-466.

Moraes, S.R., Huerta-Vilca, D., Motheo, A.J. 2004. Characteristics of polyaniline synthesized in phosphate buffer solution. *European Polymer Journal*, **40:** 2033-2041.

Ong, C.K., Ray, S., Cooney, R.P., Edmonds, N.R., Easteal, A.J. 2008. Preparation and characterization of composites of polyethylene with polypyrrole-coated wollastonite. *Journal of Applied Polymer Science*, **110:** 632-640.

Oyama, N., Tatsuma, T., Sato, T., Sotomura, T. 1995. Dimercaptan–polyaniline composite electrodes for lithium batteries with high energy density. *Nature*, **373:** 598.

Oz, K., Yavuz, M., Yilmaz, H., Unal, H.I., Sari, B. 2008. Electrorheological properties and creep behavior of polyindole/poly (vinyl acetate) composite suspensions. *Journal of Materials Science*, **43:** 1451-1459.

Patterson, A. 1939. The Scherrer formula for X-ray particle size determination. *Physical Review*, **56:** 978.

Rajasudha, G., Shankar, H., Thangadurai, P., Boukos, N., Narayanan, V., Stephen, A. 2010. Preparation and characterization of polyindole–ZnO composite polymer electrolyte with $LiClO_4$. *Ionics*, **16:** 839-848.

Rieger, K.C., Virta, R.L. 1999. Wollastonite. *The American Ceramic Society Bulletine*, **78:** 146-148.

Sainz, M., Pena, P., Serena, S., Caballero, A. 2010. Influence of design on bioactivity of novel $CaSiO_3$–$CaMg(SiO_3)_2$ bioceramics: *in-vitro* simulated body fluid test and thermodynamic simulation. *Acta Biomaterialia*, **6:** 2797-2807.

Skotheim, TA. 1986. Handbook of Conducting Polymers, vol. **1 & 2,** Marcel Dekker Inc., New York, USA.

Talbi, H., Ghanbaja, J., Billaud, D., Humbert, B. 1997. Vibrational properties and structural studies of doped and dedoped polyindole by FTIR, Raman and Eel spectroscopies. *Polymer*, **38:** 2099-2106.

Tangboriboon, N., Khongnakhon, T., Kittikul, S., Kunanuruksapong, R., Sirivat, A. 2011. An innovative $CaSiO_3$ dielectric material from eggshells by sol–gel process. *Journal of Sol-Gel Science and Technology*, **58:** 33-41.

Taylan, N.B., Sari, B., Unal, H.I. 2010. Preparation of conducting poly (*vinyl chloride*)/polyindole composites and freestanding films via chemical polymerization. *Journal of Polymer Science Part B: Polymer Physics*, **48:** 1290-1298.

Tourillon, G., Garnier, F. 1982. New electrochemically generated organic conducting polymers. *Journal of Electroanalytical Chemistry and Interfacial Electrochemistry*, **135:** 173-178.

Virta, R.L., Van Gosen, B.S. 2001. Wollastonite: A *Versatile Industrial Mineral*, 2 pp., US Geological Survey, Fact Sheet 002-01, USA.

Wang, H., Zhang, Q., Yang, H., Sun, H. 2008. Synthesis and microwave dielectric properties of $CaSiO_3$ nanopowder by the sol–gel process. *Ceramics International*, **34:** 1405-1408.

Wei, J., Chen, F., Shin, J.-W., Hong, H., Dai, C., Su, J., Liu, C. 2008. Preparation and characterization of bioactive mesoporous wollastonite–polycaprolactone composite scaffold. *Biomaterials*, **30:** 1080-1088.

Wu, H., Yang, J., Ma, H., Wang, M. 2013. Preparation of acicular wollastonite using hydrothermal and calcining methods. *Integrated Ferroelectrics*, **146:** 144-153.

Xinhai Sr, L. 2006. (70aa) Study of the preparation of ultrafine high aspect ratio wollastonite powders. *2006 AIChE The Spring National Meeting and Global Congress on Process Safety*, USA.

Zhao, W., Zhang, Q., Peng, C. 2006. FTIR spectra for molecular structure of wollastonite. *Journal-Chinese Ceramic Society*, **34:** 1137.

Zhijiang, C., Ruihan, Z., Xingjuan, S. 2012. Preparation and characterization of polyindole nanofibers by electrospinning method. *Synthetic Metals*, **162:** 2069-2074.